Determination The Effect Of Operational Loads On Residual Stresses In Dissimilar Metal Welds By Numerical Simulation

Heterogén hegesztett kötésben az üzemi terhelések maradó feszültségre gyakorolt hatásának a meghatározása numerikus szimuláció segítségével

Bernadett Spisák[a], Szabolcs Szávai[b]

[a, b]Bay Zoltán Nonprofit Ltd. for Applied Research; University of Miskolc
[a]tudományos munkatárs, bernadett.spisak@bayzoltan.hu, [b]osztályvezető, szabolcs.szavai@bayzoltan.hu

Kulcsszavak
heterogén hegesztett kötés, végeselem analízis, maradó feszültség, üzemelési terhelések

Absztrakt
A cikk egy VVER-440 gőzfejlesztőn végzett számítási eredményeket foglalja magában, ahol a heterogén hegesztett kötés mellett a primer köri körülmények is figyelembe voltak véve. A számítások magába foglalják a tranziens varrat hegesztésből származó maradó feszültségeit és az üzemelési terheléseket is. A kapott eredmények felhasználhatók a későbbiekben a feszültségkorróziós repedés keletkezési helyének a meghatározására és a hegesztett kötés élettartamának és meghibásodásának az előrejelzésére.

Keywords
dissimilar metal welding, finite element analysis, residual stress, operational loads

Abstract
This paper summarizes the computation results of residual stresses of the VVER-440 steam generator (SG) where beside the DMW the primary loop collector of the SG is also investigated. The calculations include the welding residual stresses of the DMW and the effects of the operational loads. The obtained results can be used in the prediction of initiation places of stress corrosion cracking and for the lifetime assessment and failure mode predictions of the welded joints.

Introduction

To achieve the best possible mechanical strength several welded connections are used in the nuclear industry. There are several cases where components made from different alloy systems must be connected. This type of weld is called dissimilar metal weld (DMW). The transition between the different parent materials is achieved with the usage of a buttering layer. In the power plant a common example is the joining of a ferritic low alloy steel to an austenitic stainless steel. Unfortunately, a large number of DMW joints show tendency of cracking, one of the causes of this cracking was determined to be stress corrosion cracking mechanism, where the dominating source of driving force is the residual stresses in the DMWs. Up until 2018 there were 46 majors operational PWR and BWR service cases which is relevant to ageing degradation by stress corrosion cracking focused on DMWs [1]. In case of WWER-440 DMWs are the reactor pressure vessels safe end welds, core spray nozzles, feedwater nozzles, jet pump instrumentation nozzles, and also the recirculation inlet and outlet steam generator nozzles. The life time of several existing nuclear power plants is planed to be extended, therefore, the accurate estimation of residual stresses in DMWs is necessary. Unfortunately, the direct measurement of residual stresses is difficult, consequently the usage of numerical modelling to estimate these stresses has widely spread [2, 3].

In this paper effect of the operational loads on the residual stresses in a DMW is investigated. 2D and 3D simulations were created to examine the DMW. In the first case the analysis was carried out with only the operational loads, where beside the mechanical loadings the thermal effects resulted from the operational temperatures are also included. In the second version of the calculations beside the operational loads the welding of the two material was applied without the modelling of the welding of the buttering layers. Finally, in the third case both type of welding (for the buttering layers and between the two basic material) was also implemented together with the mechanical and thermal loadings.

1. Geometry

The examined DMW can be found in the steam generator of the WWER 440MW unit. The steam generator is placed horizontally and is connected to vertical cylindrical hot and cold collectors, the schematic picture of it can be seen on Fig. 1. where the placement of the DMW is also shown.

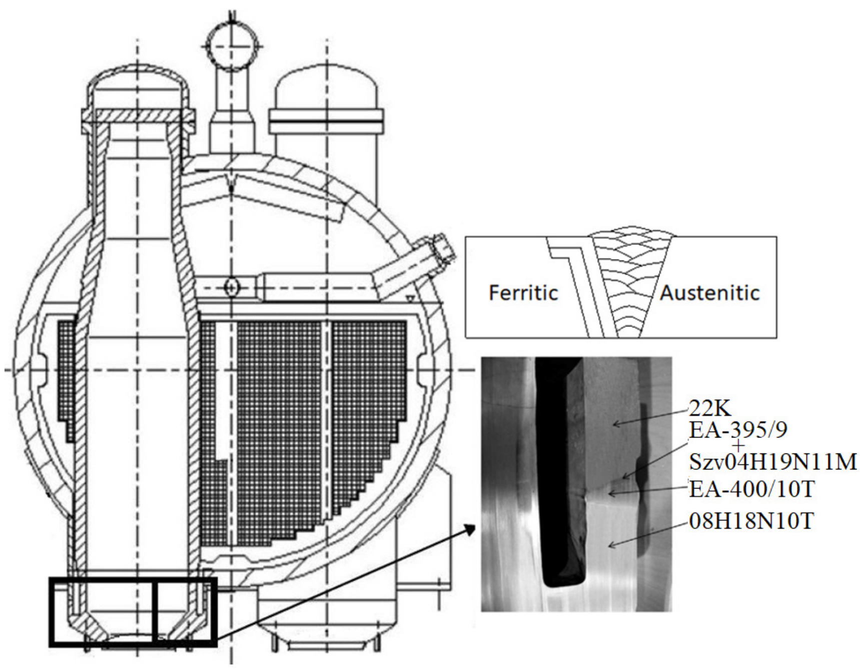

Figure 1. Schematic picture of Steam Generator

The steam generator (SG) is made from carbon steel (22K) and the collectors are manufactured from austenitic steels (08H18N10T), therefore at the connection of these components dissimilar metal welding was used. Because of the differences in the base materials the implementation of buttering layers is necessary. Here three layers were applied two high alloyed layers from EA-395/9, Sv-04CH19N11M3 and filler metal EA-400/10T and one from EA-400/10T.

2. Finite Element Simulation Built-up

Material. The material properties were calculated with the help of JMatPro softver based on the chemical compositions of the base metals. The chemical compositions are listed in Table 1.

Table 1. *Chemical compositions of the base metals*

Material	C (%)	Si (%)	Mn (%)	S (%)	P (%)	Cr (%)	Ni (%)	Cu (%)	Co (%)	Mo (%)	Ti (%)
22K	0.29	0.40	1.0	0.25	0.25	0.30	0.30	0.30	0.02	-	-
EA-395/9	0.08	0.35	1.2	-	-	13.5	23	-	0.08	4.5	-
EA-400/10T	0.07	0.5	1.5	-	-	17	9.5	-	-	2	-
08H18N10T	0.08	0.08	1.5	0.02	0.035	17	9	-	-	-	0.4

For the 22K material temperature dependent elastic-plastic isotropic hardening, phase-dependent material model was applied while for the austenitic materials the Chaboche's combined hardening law was chosen. In MSC. Marc for this hardening model at least five parameters must be given which can be determined from experimental stress vs. strain curves.

Operational loads. The finite element analysis can be separated into two main part, the first is the simulation of the welding where the material data were set as a temperature dependent variable. In case of the 3D simulation four thermal loadings were applied, to simulate the temperature of the environment, the primary collector inner surface, the stream generator inner surface and the outer surface of primary collector. The inner surface of the primary collector is set on 325°C and is heated up by the primary circuit water, the temperature applied on the outer side of it and the inner surface of the steam generator is 270°C and for every other outer surfaces the environmental temperature were set. In case of the 2D geometry the temperature of the SG inner surface was not included. Thereafter the mechanical boundary conditions were prepared, which contain the fixed displacements and the mechanical loadings. The steam generator was fixed in two directions with the usage of three point to prevent the rigid-body motion and at the same time allow the expansion of the shell and also another boundary condition was given to simulate the symmetry of the SG. The mechanical loadings contain five boundary conditions which come from the operational pressures. Two of these are shown in Fig. 2. where the 3D mesh can also be seen. The remaining three boundary conditions are placed at the end of the steam generator nozzle, the primary collector and the steam generator shell. For the 2D simulation lesser number of boundary condition was implemented.

Welding. The simulation altogether contains 124 welds which can be seen on Fig. 3. In case of the 2D geometry all of them were modelled with the usage of Goldak's double ellipsoid heat source shape where the estimation of the heat source shape parameters was done based on the literature and the welding procedure specification. The most important welding parameters are listed in Table 2.

Table 2. *Welding parameters of the claddings and the joining weld*

	Welding run	Material	Welding process	Current [A]	Voltage [V]	Type of Current and Polarity	Heat Input [kJ/mm]
Cladding 1	1-15	EA-395/9	111	125-135	24-25	DCEP	0.61
	16-45	EA-400/10T	111	140-150	25-26	DCEP	0.69
Cladding 2	1-11	EA-395/9	111	125-135	24-25	DCEP	0.61
	12-36	EA-400/10T	111	140-150	25-26	DCEP	0.69
Joining weld	1	08H18N10T	141	70-80	24-25	DCEN	0.61
	2-43	08H18N10T	111	140-150	25-26	DCEP	0.69

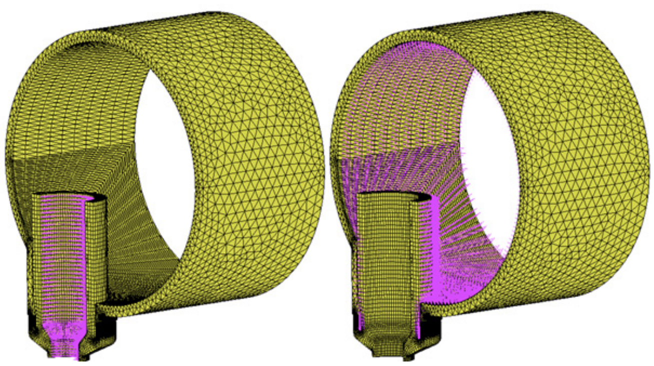

Figure 2. *Location of pressure loads (primary circuit left side, secondary circuit right side)*

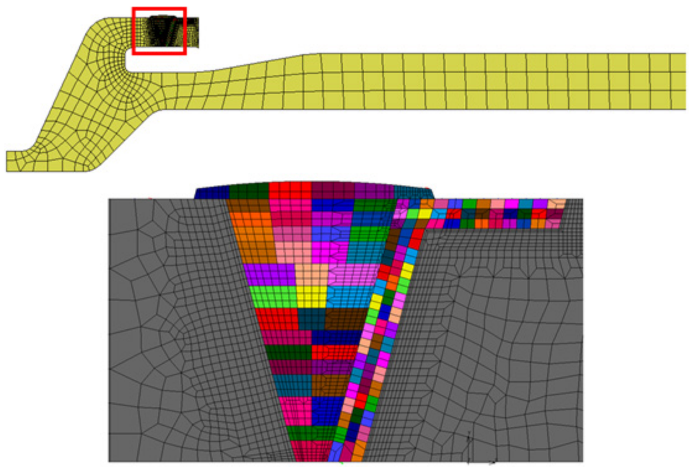

Figure 3. *2D mesh and placement of welds*

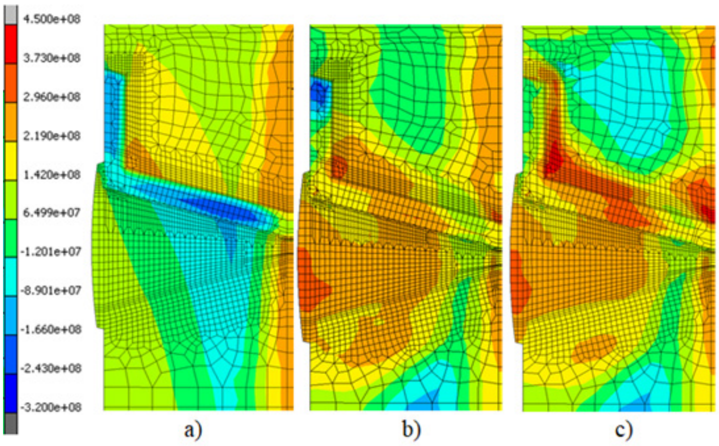

Figure 4. Computed hoop stress [Pa] after operational loading for the 3D model a) without welding, b) with joining welding, c) complete welding

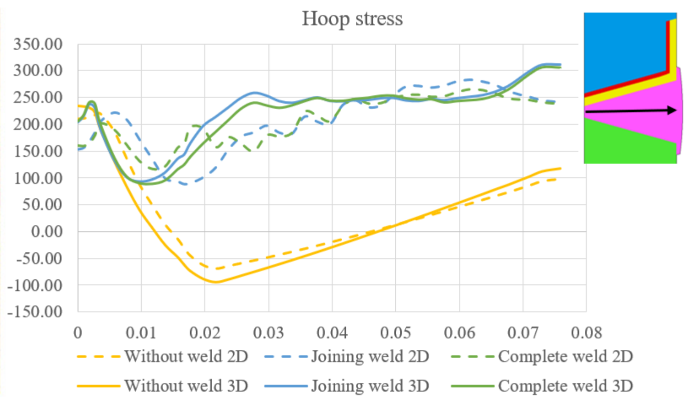

Figure 5. Hoop stress alteration in the middle of the joining weld

As a dissimilar metal weld between the base materials a transient cladding had to be implemented. This cushion has three layers. After finishing the cladding post weld heat treatment was not applied.

The surface heat losses were simulated with the help of thermal edge (face for 3D) films which were applied on the free surfaces with a heat transfer coefficient (20W/mK) for the convective heat loss and a emissivity coefficient ε=0.8 for the radiation heat loss. In case of the 3D model the initial condition mapping tool was applied to map the data of residual stresses fields from the 2D simulation on the 3D analysis.

3. Results of the simulations

As the purpose of this research was the estimation of the operational loadings effects on the residual stresses therefore in the followings the distribution of the stresses are introduced more deeply. The DMWs in the steam generator of WWER 440 has a tendency of cracking on the boundary of the ferritic and austenitic material therefore the inspection of this part of the DMW must be completed. Fig 4. shows the computed hoop stresses in case of the 3D model. The results are taken out from the middle of the circumference. The first picture (a) presents the hoop stresses resulted from the operational loads without the simulation of the welding. At the boundary of the cladding and the ferritic base metal there is a difference in the stress distribution which is also noticeable in the version made with welds. Furthermore, it is also important to recognize the differences between the second and third pictures, where the analysis differ in the simulation of the buttering layers. It is observable that in case of the modelling of the whole welding procedure the arising hoop stresses are higher at the boundary of the ferritic and austenitic material and also the highest stress values are located here too.

Fig. 5. shows the hoop stresses [MPa] along the middle of the joining weld. The diagram contains the 2D and 3D results. The differences in the values received from the 2D simulations come from the different applied boundary conditions as the pressure at the inner surface of the second circuit could not be applied, however it is seeable that much higher stresses arises in the structure when the simulation of the welding are included. Therefore, from the results it can be seen that residual stresses originated from the welding can not be neglected.

Fig. 6. and Fig. 7. shows the axial stresses distribution. From the pictures it can be seen that the simulation of the welding has lower effects on the residual stresses,

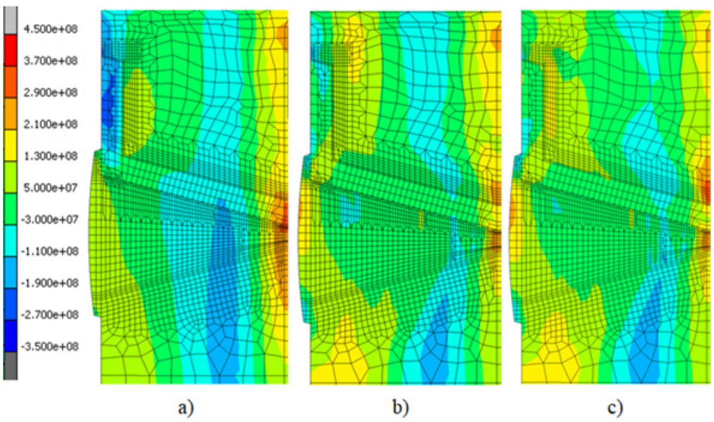

Figure 6. Computed axial stress [Pa] after operational loading for the 3D model a) without welding, b) with joining welding, c) complete welding

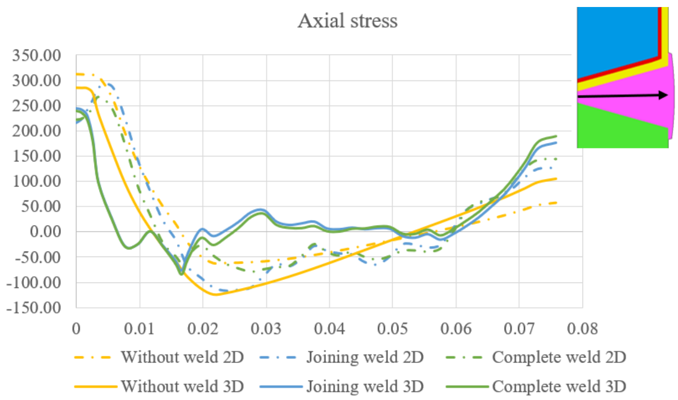

Figure 7. Axial stress alteration in the middle of the joining weld

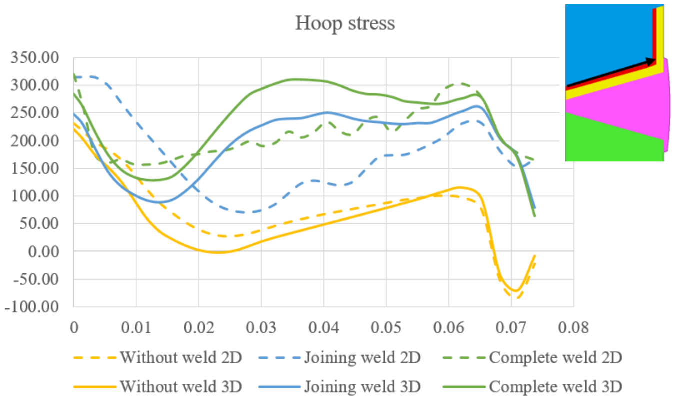

Figure 8. *Hoop stress alteration at the boundary of ferritic and austenitic material*

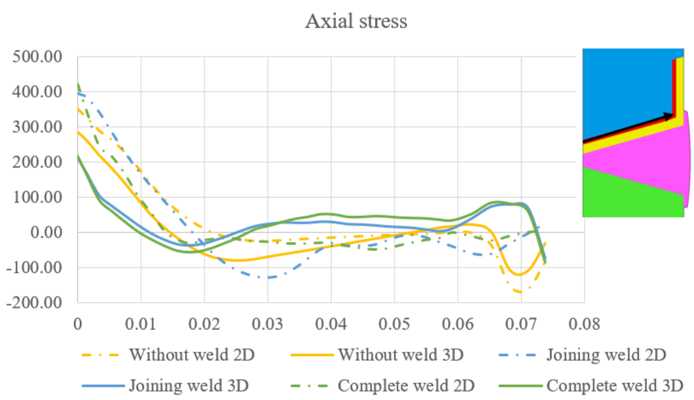

Figure 9. *Axial stress alteration at the boundary of ferritic and austenitic material*

however at the boundary of the ferritic material and the buttering layer high tensile axial stresses arise therefore at this place the weld will have a high sensitivity to SCC.

Fig. 8. and Fig. 9. shows the computed hoop and axial stresses in MPa which goes along the boundary between the ferritic base metal and the first austenitic buttering layer. As in the previous cases too the stresses without the simulation of welds is highly different from the simulations which includes the welds. As the boundary conditions applied for the 2D and 3D analysis is not completely the same therefore in the results some diversion can be observed however from both cases it can be noticed that with the simulations of the buttering layers the occurring stresses increased therefore the simulation of the buttering layers should not be neglected. However it has to be taken into account that in reality the buttering layers in the steam generator DMWs were post weld treated after the buttering therefore in the future farther simulations are necessary to determine the real stress distribution in the welding where the effect of creep and post weld heat treatment are also included.

4. Summary

The numerical simulation of dissimilar metal weld of a steam generator was introduced in this work, where the buttering layer welds, and the joining welds were also modeled. The purpose of the research was to determine the effects of operational loads on the residual stresses. Three scenarios were taken into consideration first the applying of the operational loads without the welding, secondly simulation of the joining welds and finally the welding of the buttering layers was also included. The following conclusions can be drawn:

1. Beside the dissimilar metal joining welding the buttering process also have significant effect on the distribution of the residual stress.
2. At the boundary of the ferritic and austenitic material on the inner side of the welding a large tensile axial residual stress appears, which can lead to a high sensitivity to SCC.
3. The axisymmetric model gives proper results if the geometry and the boundary condition are set adequately.

Acknowledgements

The project and this publication was supported by the Thematic Excellence Programme 2020.

References

[1] International Atomic Energy Agency, Dissimilar Metal Weld Inspection, Monitoring and Repair Approaches IAEA-TECDOC-1852, IAEA, Vienna, 2018.

[2] M. L. Benson, P. A. C. Raynaud, J. S. Wallace, Exploring finite element validation for weld residual stress prediction, Proceedings of the ASME 2018 Pressure Vessels and Piping Conference. Volume 6B: Materials and Fabrication. Prague, Czech Republic. July 15–20, 2018.

[3] Z. Bézi, Sz. Szávai, Repair Weld Simulation of Austenitic Steel Pipe, Advanced Materials Research, 1029 (2014) 194–199.